Functional Design and Prototyping of a Novel Soft Fingertip with Variable Stiffness

Functional Design and Prototyping of a Novel Soft Fingertip with Variable Stiffness

Giovanni Colucci, Carmen Visconte and Giuseppe Quaglia

Abstract The paper presents a novel soft fingertip for soft robotics application in greenhouses and protected cultivation. The system is designed to be easily adapted to different commercial end-effectors while not compromising their functionalities. The use of auxiliary vessels with combined air and liquid presence allows the adjustment of the fingertip stiffness to guarantee different values of exerted contact force and stiffness when compressed. A simplified design method to evaluate the influence of the membrane shape and the set-up parameters on the system behavior is reported. The method was compared with experimental measurements on a first system prototype.

Key words: SDG12, Assistive Robotics, Soft Fingertip, Compliant Grasping

1 Introduction

Within the last decades, Precision Agriculture (PA) has become a highly productive research field thanks to its significant impact in helping human being for responsible and intelligent crops farming [9, 2, 12]. The academic research in PA technologies and methods pursues the 2030 Agenda for Sustainable Development, especially the Sustainable Development Goal (SDG) 12 towards sustainable consumption and production patterns. Robotic systems and technologies are nowadays also implemented in protected cultivation, where the crops are preserved from environmental and external factors, e.g. precipitation and pests, and a high level of cultivation control is guaranteed to address the constant worldwide population growth and rise in food demand [7, 4]. These scenarios are often exploited for the mass production of highly-

Giovanni Colucci, Carmen Visconte and Giuseppe Quaglia
Department of Mechanical and Aerospace Engineering, Politecnico di Torino, Corso Duca degli Abruzzi 24, Torino 10129, ITALY, e-mail: {giovanni_colucci; carmen.visconte; giuseppe.quaglia}@polito.it

valued cultivation, where the process automation and mechanization helps for heavy and repetitive tasks.

In protected cultivation, the most time-consuming and intensive activity is usually harvesting [4], and several solutions based on mechanical harvesting, shake-and-catch systems or selective methods have been investigated. Besides, the target fruit is often too fragile and delicate to be grasped with rigid robotic hand, thus the use of compliant and soft grasping interfaces are often proposed for tomatoes [3], sweet peppers [10, 7] and strawberries [5]. Soft materials are widely studied because of their adaptability and to not leave damages or even signs on the grasped object [6]. In [8] an anthropomorphic fingertip made by silicone rubber and distributed internal strain gauges is presented, where the sensors are not calibrated and the grasping model is built on experimental data. In [1] a similar fingertip structure is used to develop a manipulator controller that adjusts the grasping stiffness. In [11] a novel contact model for silicone-made fingertip was presented, where the classical rigid fingertip approach is changed to take into consideration the membrane deformation.

In this paper, a novel soft fingertip with variable stiffness for autonomous picking is presented. It is based on a combined hydraulic and pneumatic auxiliary vessels, and it is designed to be adapted to different commercial robotic end-effectors just changing the fingertip mounting base geometry (Fig. 1) without compromising the robotic manipulator functionalities.

2 Functional design

The novel fingertip under investigation is based on a soft membrane, whose structural stiffness is ideally negligible when pressed, connected to an auxiliary hydraulic/pneumatic system that determines the variable stiffness behaviour. Thus, as presented in Fig. 2, the system functional architecture is based on the following components:

(a) **(b)**

Fig. 1 **(a)** The proposed soft fingertip mounted on a commercial KinovaGen2 manipulator. **(b)** Behaviour of the soft fingertip when grasping a generic object.

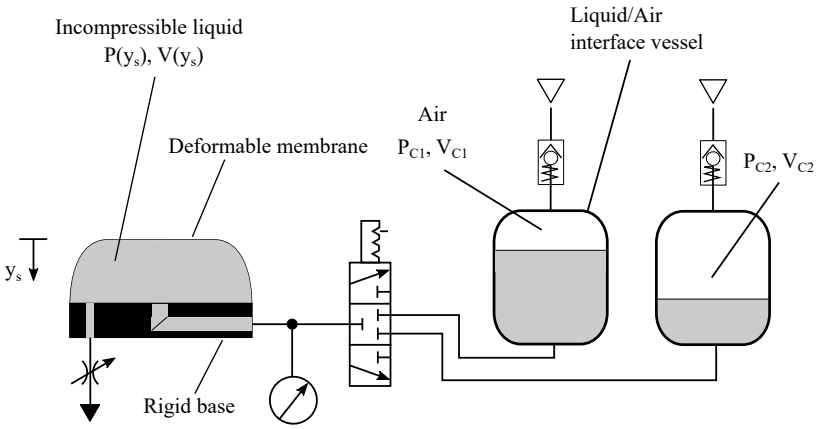

Fig. 2 System functional architecture.

- The soft membrane itself;
- A rigid mounting base, that is also demanded to connect the membrane volume to the auxiliary system;
- Two auxiliary volumes that are respectively under the absolute pressure levels P_{C1}, P_{C2}. They are partially filled with the same incompressible liquid that is within the membrane, and the remaining volume, that is respectively V_{C1}, V_{C2} is filled with air;
- A 3/3 digital valve that regulates the possible connections between the fingertip and the two auxiliary volumes;

If the dynamic behaviour of the proposed architecture is neglected, the liquid that fills the fingertip volume V acts as an hydrostatic transmission when the fingertip is compressed of a y_s value, and it provokes the compression of the V_{C1}, or V_{C2}, air volume. Thus, the resulting fingertip stiffness is mainly related to the compression law of the air volume, that can be adjusted by setting the initial value of the pressure level $P_{C[1,2],i}$ and air volume $V_{C[1,2],i}$. In particular, this feature would be used to achieve two different behaviour of fingertip stiffness, where the first one should be used to manipulate and grasp soft and delicate objects, while the second one should be used for rigid ones.

Moreover, the 3/3 valve also allows to disconnect V from both the auxiliary volumes. In this case, even a low value of y_s causes a significant increment of the exchanged contact force F, since the fingertip stiffness is now imposed by the fluid compressibility and the membrane deformability, that are no longer negligible.

Regarding the additional components, the two non-return valve connected to the auxiliary reservoirs $V_{C,[1,2]}$ are used to connect the supply pressure source during the set-up procedure. A flow control valve is mounted on the rigid base to allow the correct spillage of air during the filling procedure of the membrane with the incompressible liquid. To complete the basic system architecture, a pressure sensor measures the pressure level P within the fingertip. As it will be presented within the

next sub-sections, this value is used to estimate the membrane compression y_s while the fingertip is in contact with the target object.

2.1 Fingertip Geometry Modelling

The obtain a geometry that is similar to a fingertip, the membrane was modelled starting from the combination of three tangent circle arcs, that lie into the first quadrant of the $< x, y >$ plane of Fig. 3. The membrane shape is then described by the radius lengths $r_{[1,2,3]}$ and arc angles $\alpha_{[1,2,3]}$. Besides, the design parameters i, h, s respectively impose the fingertip width, length and thickness. It is worth underlining that, while i could be imposed by the specific fingertip application, e.g. its implementation on a robotic manipulator end-effector with specific geometries, h and s can be varied during the design process. As presented in section 3, s mainly affects the fabrication procedures, since it could be difficult to produce excessively thin membrane but the fingertip structural stiffness would increase if a too high value of s is selected. On other hand, the height h changes the maximum compression length $y_{s,max}$, i.e. it changes the total amount of volume ΔV that can be squeezed while manipulating the target object.

To obtain the entire fingertip geometry, the described shape is flipped around the y axis and extruded by the length l along z. The volumes at the extremities that complete the membrane are then obtained as solids of revolution around the same y axis. Please notice how l depends on L according to the following equation:

$$L = l + 2i \tag{1}$$

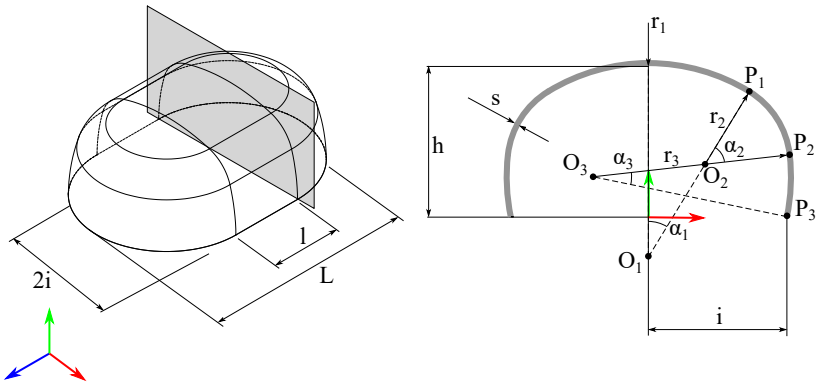

Fig. 3 **(a)** membrane axonometric view. **(b)** Section view of the membrane

The geometric constraints, i.e. the vertical displacement of O_1, the tangency between the consecutive arcs and the horizontal displacement of the end point of the arc of radius r_3, reduce the number of geometric parameters down to four values. Thus, a selected number of possible type of shapes were classified by varying four adimensional parameters, that are compared with the two encumbrance parameters i and h, as reported in Tab. 1. The four selected shapes are also depicted in Fig. 4:

- In Type A case, almost the entire horizontal encumbrance i is reached by the first arc portion of radius r_1, while the third arc presents minimal curvature, i.e. $r_3 >> r_1$.
- Type B case has the three arc radius quite similar between them, i.e. $r_1 \simeq r_2 \simeq r_3$. Thus, it represents the shapes that reproduce a spherical membrane within the $< x, y >$ plane.
- Type C represents the category of membrane where r_1 arc has an high value of α_1, i.e. $\alpha_1 \geq \pi/3$, and the remaining arcs with a minimal curvature.
- In Type D case, the r_1 arc reaches the entire encumbrance , i.e. $x_{P1} \approx i$, thus producing a bellow-like geometry.

2.2 Fingertip Stiffness Estimation

The selection of a membrane shape among the four presented types produces significant effects on the system properties, especially in terms of grasping force F. Within the present subsection, a simplified model of the fingertip compression while manipulating is presented. To this aim, the following simplifying assumptions are made:

- The grasped object is considered as infinitely rigid, then the fingertip is the only part between the two that is subject to deformation;
- The grasped object is considered as planar, i.e. it can be modelled as a plane that covers the entire fingertip encumbrance within the $< x, z >$ plane;
- The deformed membrane is not subjected to radial deformation, i.e. each $< x, z$ membrane section does not elongate or contract.

The last two assumptions lead to a deformed fingertip geometry that is obtained by sectioning the membrane with a plane that is parallel to $< x, z >$. Thus, as

Table 1 Adimensional parameters for the shape types presented.

Type	$a = \frac{x_{P1}}{i}$	$b = \frac{y_{P1}}{h}$	$c = \frac{x_{P2}}{x_{P1}}$	$d = \frac{y_{P2}}{y_{P1}}$
Type A	0.65	0.9	1.4	0.7
Type B	0.85	0.55	1.02	0.95
Type C	0.57	0.7	1.4	0.5
Type D	0.6	0.95	1.7	0.8

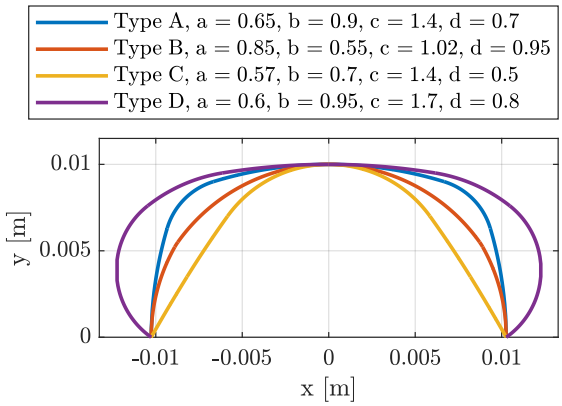

Fig. 4 Section view of the four types of membrane shapes in the $< x, y >$ plane.

presented in Fig. 5, the two functions of internal volume V and contact area A are only functions of the compression length y_s and can be obtained once the membrane geometry is known. The proposed considerations could result as too simplifying when manipulating complex geometries and/or objects that are smaller than the fingertip, also it doesn't consider the border effect near the contact area and those near the base mounting. Nevertheless it is worth underlining that they were introduced to have an effective design methodology to get a first estimation of the system behaviour that must be still compared with experimental measurements.

When the fingertip is subject to a compression equal to y_s, the air volume trapped into the first (or second) auxiliary vessel is therefore equal to:

$$V_{C1} = V_{C1,i} - \Delta V(y_s) \tag{2}$$

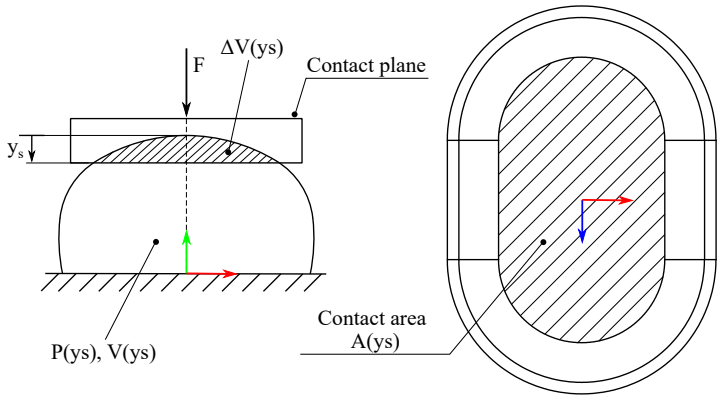

Fig. 5 Model of the fingertip when compressed by a planar and infinitely rigid object.

where $V_{C1,i}$ is the initial air trapped volume, that can be adjusted during the system set-up procedure, and ΔV is the amount of liquid that is squeezed from the fingertip into the auxiliary system. By referring to V_i, that is the initial incompressible liquid volume within the fingertip, the adimensional ξ_{C1} parameter can be introduced:

$$\xi_{C1} = \frac{V_{C1,i}}{V_i} \tag{3}$$

By assuming that the air volume comes under an adiabatic transformation ($\gamma = 1.4$), the absolute pressure P inside the fingertip will follow the standard compression rule:

$$P(y_s) = P_{C1,i}\left(\frac{V_{C1,i}}{V_{C1,i} - \Delta V(y_s)}\right)^{\gamma} \tag{4}$$

Thus, the exerted contact force F can be defined as the product between the relative pressure $p = P - P_{atm}$ and the contact area $A = A(y_s)$:

$$F = p(y_s)\, A(y_s) \tag{5}$$

and the obtained stiffness can be defined as follows:

$$k(y_s) = \frac{dF(y_s)}{dy_s} = p(y_s)\frac{dA(y_s)}{dy_s} + \frac{dp(y_s)}{dy_s}A(y_s) \tag{6}$$

that highlights how both the geometrical parameters, i.e. the contact area and the compression transformation, affect the overall system stiffness.

By taking into account Equation 2 and Equation 4, k can be computed as:

$$\begin{aligned} k(y_s) = \quad & \left(P_{C1,i}\left(\frac{V_{C1,i}}{V_{C1,i}-\Delta V(y_s)}\right)^{\gamma} - P_{atm}\right)\frac{dA(y_s)}{dy_s} + \\ & - \gamma\, P_{C1,i}\, \frac{{V_{C1,i}}^{\gamma}}{(V_{C1,i} - \Delta V(y_s))^{\gamma+1}}\, \frac{d\Delta V(y_s)}{dy_s}\, A(y_s) \end{aligned} \tag{7}$$

where the geometric features of the membrane affect k in terms of the squeezed incompressible liquid volume ΔV, the contact area A and their first order derivatives. The two initial values $P_{C1,i}$ and $V_{C1,i}$ can instead be used as set-up parameters to adjust the stiffness curve.

The estimated behaviour of F for the four geometrical types was then obtained by assuming the values of the set-up parameters, as presented in Fig. 6. Type A and Type D present a high stiffness for low value of y_s due to the first term of Equation 6. Type C presents the lowest value of F, even though the ending part of its graph presents an increasing value of stiffness due to the second term of Equation 6 .

Nevertheless, the model doesn't consider the border effects that depend on the base-membrane constraints and the membrane thickness, that don't allow the total fingertip compression if the membrane folds on itself when compressed. Thus, it is reasonable to assume a maximum compression value that is lower than the total height $y_{s,max} < h$. In Fig. 6, a maximum value of $y_{s,max} = 7.5$ mm was used.

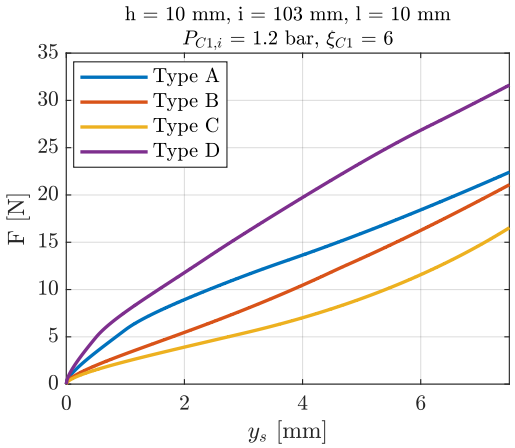

Fig. 6 Contact force F for all types of membrane shape.

3 Prototyping and Experimental Tests

To validate the novel sensing system through experimental tests, a first version of the fingertip was produced in laboratory environment by using standard and affordable technologies and materials for soft robotics applications. The fingertip membrane was both manufactured in addition cure silicone rubber by casting processes but also in thermoplastic polyurethane by FDM (fused deposition modeling) technologies. To this aim, Type A shape was selected for its higher value of contact force F for fixed y_s, while Type D shape resulted as too difficult to manufacture.

Regarding the silicone membrane, the moulds were realized in plastic material (PLA) with an FDM printer. The membrane internal structure was strengthened with cotton filaments which prevent the membrane expansion when inflated. As showed in Fig. 7 (a), different values of thickness s were tested with the same material in order to evaluate the membrane stiffness. According to the authors' experience, it is possible to produce these shape with thickness values down to 1 mm while maintaining the procedures quite simple and easy to reproduce. On other hand, even though an higher value of s results into easier manufacturing procedures, the resulting membrane structural stiffness resulted as too high for the specific application. Moreover, due to the thinness of the membrane, it resulted as fundamental the implementation of degassing procedures to avoid the inclusion of air bubbles inside the structure.

With regards to the use of a rapid prototyping printer, the use of FDM techniques allows to realize a single-piece fingertip that both includes the membrane and the rigid base itself, but the use of supporting material for the membrane is not allowed due to the closed shape of the fingertip. The authors tested only a TPU 95A material that was printed with s= 1 mm, but it resulted as to rigid. It is worth underlining how a lower value of s was not possible since it resulted into liquid leakages. The authors don't prevent the possibility to obtain a proper and soft membrane with the use of different nozzle diameters and different materials.

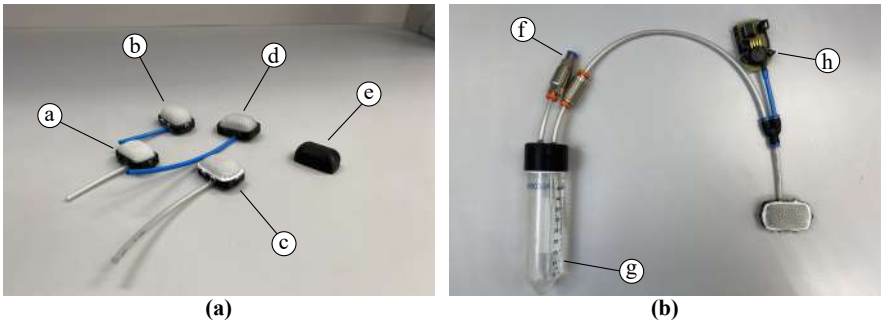

(a) **(b)**

Fig. 7 **(a)** Produced membranes with different materials and thickness. a: EcoFlex 00-50 s = 1 mm, b: EcoFlex 00-50 s = 2 mm, c: EasyComposites AS40 s = 1 mm, d: EasyComposites AS40 s =2 mm, e: TPU 95A s=1 mm. **(b)** Overview of the entire system with auxiliary components. f: mon return supply-valve, g: ElveFlow microfluidic reservoir, h: pressure sensor.

For all the presented shapes and materials, an experimental evaluation of the membrane structural stiffness was carried out and summarized in Tab. 2 by reporting only the average stiffness $k_{struct,avg}$, defined as the ratio between the maximum force and the related compression value that were measured before the start of the border effects:

$$k_{struct,avg} = \frac{F_{max}}{y_{s,max}} \tag{8}$$

The auxiliary vessels (in Fig. 7(a) a single-auxiliary-volume V_{C1} is presented) were realized by using a 50 mL microfluidic reservoir with a custom two-holes cup, where the first is used for the external air pressure supply and the latter to catch the liquid from the middle of the vessel by means of an internal tube.

The silicone-made membrane needs a fixing system to mount it upon the rigid base, that was realized with plastic PLA material, and prevents from liquid leakages. In Fig. 8 an exploded view of the fingertip sub-system is presented. Please notice how the sealing functionality is guaranteed by a cone mounting, since both the base and the ring sides are inclined of a certain angle, then the mounting screws only guarantee the correct positioning of the ring with respect to the base. On the bottom of the membrane, a screw was added to realize the air spillage during the set-up filling of the fingertip.

Table 2 Average structural stiffness for the tested materials and thickness values.

Material	Thickness	$k_{struct,avg}$ [N/mm]
EcoFlex 00-50	1 mm	0.82
EcoFlex 00-50	2 mm	1.01
EasyComposites AS40	1 mm	1.56
EasyComposites AS40	2 mm	4.10
FDM TPU 95A	1 mm	7.35

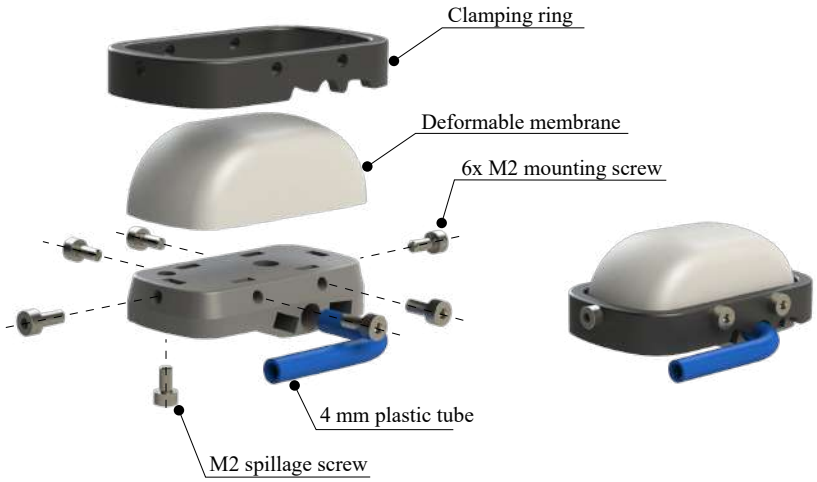

Fig. 8 Exploded view of the fingertip mounting system.

3.1 Experimental Evaluation of Fingertip Contact Force

Within the present subsection, the experimental measurements of the contact exerted force between the fingertip and a planar and infinitely rigid object are presented. The membrane made of AS40 silicone rubber and 1 mm thick was selected, since it still presents a relatively low structural stiffness value but also the AS40 material resulted as more resistant to abrasion and wear than the EcoFlex 00-50.

The results of the experimental measurements are showed in Fig. 9 for a couple of set-up parameters that are equal to $\xi_{C1} = 3.52$ and $P_{C1,i} = 1.2$ bar. The measure-

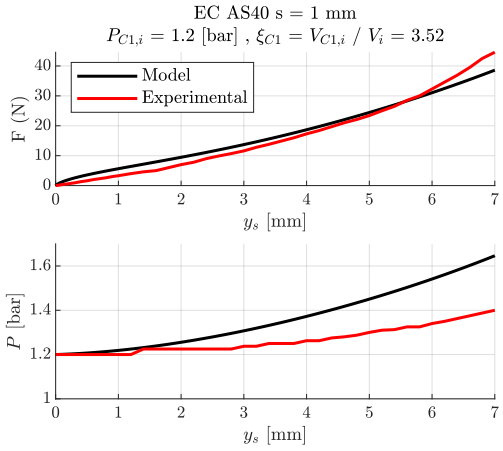

Fig. 9 Model and experimental curves of contact force and internal pressure for a fixed set-up of design parameters.

ments were done up to a compression of $y_s = 7$ mm since the membrane thickness and the clamping ring don't allow bigger value of y_s. The simplified model overestimates the contact force F until the value of $y_s \approx 5.5$ mm is reached, where a crossing point between the model and the experimental curve occurs. The model underestimates also the fingertip internal pressure for all the compression range, with a final (and maximum) gap of 0.24 bar (17% of relative error). This behaviour is mainly related to the assumption of no membrane expansion within the $< x, z >$ plane.In fact, the membrane undergoes the bending of its sides when compressed (Fig. 10), leading to lower values of $P(y_s)$. Lastly, the crossing point in the exerted force graph is caused by the increase of structural stiffness due to the fingertip border effects.

4 Conclusion

The paper presented a novel deformable fingertip for precision agriculture applications in greenhouses, where an auxiliary system is demanded to adjust the stiffness and exerted contact force behaviour as a function of the fingertip compression. A simplified model, based on the assumption of homogeneous membrane deformation and planar contact, was used to design the membrane geometry and to choose the set-up parameters, i.e. initial pressure and air trapped volume.

The employed manufacturing process was described in terms of adopted technologies and materials, underlining how it results as affordable and easy to reproduce even in laboratory environment. Additional details about the thickness value choice, the materials and the fingertip custom-made system were presented, also in terms of resulting membrane structural stiffness.

Experimental measurements on a selected membrane shape and material were carried out, that proved the effectiveness of the simplified methods for designing purposes but also highlighted how an experimental system characterization is fundamental to not overestimate the membrane internal pressure.

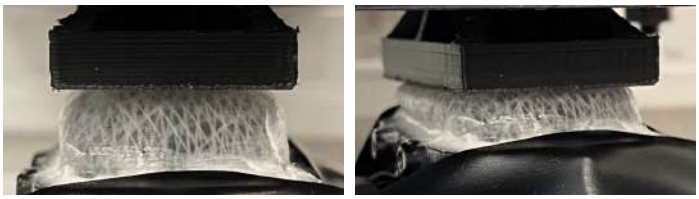

(a) **(b)**

Fig. 10 **(a)** Fingertip at the beginning of the compression test. **(b)** Fingertip under compression.

References

1. Biagiotti, L., Tiezzi, P., Vassura, G., Melchiorri, C.: 4 modelling and controlling the compliance of a robotic hand with soft finger-pads. Multi-point Interaction with Real and Virtual Objects pp. 55–73 (2005). https://doi.org/10.1007/11429555_4
2. Bongiovanni, R., Lowenberg-Deboer, J.: Precision agriculture and sustainability. Precision Agriculture **5**(4), 359–387 (2004). https://doi.org/10.1023/B:PRAG.0000040806.39604.aa
3. Chiu, Y.C., Chen, S., Lin, J.F.: Study of an autonomous fruit picking robot system in greenhouses. Engineering in Agriculture, Environment and Food **6**(3), 92–98 (2013). https://doi.org/10.1016/S1881-8366(13)80017-1
4. Davidson, J., Bhusal, S., Mo, C., Karkee, M., Zhang, Q.: Robotic manipulation for specialty crop harvesting: A review of manipulator and end-effector technologies. Global Journal of Agricultural and Allied Sciences **2**(1), 25–41 (2020). https://doi.org/10.35251/gjaas.2020.004
5. De Preter, A., Anthonis, J., De Baerdemaeker, J.: Development of a robot for harvesting strawberries. IFAC-PapersOnLine **51**(17), 14–19 (2018). https://doi.org/10.1016/j.ifacol.2018.08.054
6. Elango, N., Faudzi, A.A.M.: A review article: investigations on soft materials for soft robot manipulations. The International Journal of Advanced Manufacturing Technology **80**(5), 1027–1037 (2015). https://doi.org/10.1007/s00170-015-7085-3
7. van Henten, E.J., Bac, C.W., Hemming, J., Edan, Y.: Robotics in protected cultivation. IFAC Proceedings Volumes **46**(18), 170–177 (2013). https://doi.org/10.3182/20130828-2-SF-3019.00070
8. Hosoda, K., Tada, Y., Asada, M.: Anthropomorphic robotic soft fingertip with randomly distributed receptors. Robotics and Autonomous Systems **54**(2), 104–109 (2006). https://doi.org/10.1016/j.robot.2005.09.019
9. Kumar, S.A., Ilango, P.: The impact of wireless sensor network in the field of precision agriculture: A review. Wireless Personal Communications **98**(1), 685–698 (2018). https://doi.org/10.1007/s11277-017-4890-z
10. Lehnert, C., English, A., McCool, C., Tow, A.W., Perez, T.: Autonomous sweet pepper harvesting for protected cropping systems. IEEE Robotics and Automation Letters **2**(2), 872–879 (2017). https://doi.org/10.1109/LRA.2017.2655622
11. Lu, Q., Rojas, N.: On soft fingertips for in-hand manipulation: Modeling and implications for robot hand design. IEEE Robotics and Automation Letters **4**(3), 2471–2478 (2019). https://doi.org/10.1109/LRA.2019.2906544, conference Name: IEEE Robotics and Automation Letters
12. Meshram, A.T., Vanalkar, A.V., Kalambe, K.B., Badar, A.M.: Pesticide spraying robot for precision agriculture: A categorical literature review and future trends. Journal of Field Robotics **39**(2), 153–171 (2022). https://doi.org/10.1002/rob.22043